



**University of
Zurich**^{UZH}

**Zurich Open Repository and
Archive**

University of Zurich
University Library
Strickhofstrasse 39
CH-8057 Zurich
www.zora.uzh.ch

Year: 2007

Spatial unmixing of MERIS data for monitoring vegetation dynamics

Zurita-Milla, Raúl ; Kaiser, Georg ; Clevers, J G P W ; Schneider, Werner ; Schaepman, Michael E

Abstract: Monitoring vegetation dynamics is fundamental to improve Earth systems models and to increase our understanding of the terrestrial carbon cycle and the interactions biosphere-climate. Medium spatial resolution sensors, like MERIS, have a great potential to study these dynamics at regional/global scales. However, the spatial resolution provided by MERIS (300m in full resolution mode) might not be appropriate over highly heterogeneous landscapes. This is why the synergistic use of MERIS full resolution (FR) and Landsat TM data is studied in this paper. An unmixing-based data fusion approach was applied to a time series of MERIS FR images acquired over the Netherlands in 2003. The selected data fusion approach uses the linear mixing model and the information derived from Landsat TM imagery acquired in the same year to produce images that have the spectral and temporal resolutions provided by MERIS but with the spatial resolution of Landsat TM. After the fusion, a quantitative assessment of the quality of the fused images was done in order to assess the validity of the proposed methodology and to evaluate the radiometric characteristics of the images. Finally, the time series of fused images was used to compute land cover specific NDVI, MTCI and MGVI profiles.

Posted at the Zurich Open Repository and Archive, University of Zurich

ZORA URL: <https://doi.org/10.5167/uzh-77413>

Conference or Workshop Item

Published Version

Originally published at:

Zurita-Milla, Raúl; Kaiser, Georg; Clevers, J G P W; Schneider, Werner; Schaepman, Michael E (2007). Spatial unmixing of MERIS data for monitoring vegetation dynamics. In: Envisat Symposium 2007, Montreux (CH), 23 April 2007 - 27 April 2007. European Space Agency * Communication Production Office, online.

SPATIAL UNMIXING OF MERIS DATA FOR MONITORING VEGETATION DYNAMICS

R. Zurita-Milla⁽¹⁾, G. Kaiser⁽²⁾, J.P.G.W. Clevers⁽¹⁾, W. Schneider⁽²⁾ and M.E. Schaepman⁽¹⁾

⁽¹⁾ Centre for Geo-Information (CGI), P.O. Box 47, 6700 AA, Wageningen University, NL – 6700 AA Wageningen, The Netherlands. Email: {Raul.Zurita-Milla, Jan.Clevers, Michael.Schaepman} @wur.nl

⁽²⁾ Institute of Surveying, Remote Sensing and Land Information, University of Natural Resources and Applied Life Sciences, 1190 Vienna, Austria. Email: {Georg.Kaiser, Werner.Scheider} @boku.ac.at

ABSTRACT

Monitoring vegetation dynamics is fundamental to improve Earth systems models and to increase our understanding of the terrestrial carbon cycle and the interactions biosphere-climate. Medium spatial resolution sensors, like MERIS, have a great potential to study these dynamics at regional/global scales. However, the spatial resolution provided by MERIS (300m in full resolution mode) might not be appropriate over highly heterogeneous landscapes. This is why the synergistic use of MERIS full resolution (FR) and Landsat TM data is studied in this paper.

An unmixing-based data fusion approach was applied to a time series of MERIS FR images acquired over the Netherlands in 2003. The selected data fusion approach uses the linear mixing model and the information derived from Landsat TM imagery acquired in the same year to produce images that have the spectral and temporal resolutions provided by MERIS but with the spatial resolution of Landsat TM.

After the fusion, a quantitative assessment of the quality of the fused images was done in order to assess the validity of the proposed methodology and to evaluate the radiometric characteristics of the images. Finally, the time series of fused images was used to compute land cover specific NDVI, MTCI and MGVI profiles.

1. INTRODUCTION

1.1. Vegetation dynamics

Monitoring vegetation dynamics is essential to better understand how the Earth system is responding to anthropogenic activities. For instance, knowledge on vegetation dynamics is fundamental to fully understand the terrestrial carbon cycle and the interactions biosphere-climate. Earth observation satellites provide regular and synoptic data that can be used to monitor these dynamics. Time series of satellite vegetation indices are commonly used to enhance the vegetation signal and to derive key phenological metrics like the day of green-up, maturity or vegetation senescence. Low and medium spatial resolution data, like the one provided by the AVHRR and MODIS sensors, are used to derive such metrics at a global scale because of their

high temporal resolution. However, an accurate characterization of vegetation phenology in heterogeneous landscapes might require higher spatial resolution data. Landsat TM could be used over this kind of landscapes but its temporal resolution (revisit time 16 days) is not very suited for monitoring purposes. Therefore, data fusion of medium and high spatial resolution sensors might be very useful to monitor vegetation phenology over heterogeneous landscapes.

1.2. Data fusion

Current Earth observation satellites provide data at a wide range of spatial, spectral and temporal resolutions. In remote sensing, data fusion deals with the combination of the data provided by two or more of the sensors aboard Earth observation satellites [1]. Fused images usually have more information than each of the input images alone [2].

In this study, an unmixing-based data fusion approach was selected to combine Landsat TM and MERIS full resolution (FR) data because this approach tries to preserve the spectral information of the low resolution image as much as possible [3]. This should facilitate the extraction of quantitative information from the fused images.

2. MATERIALS AND METHODS

2.1. Study area and datasets

The study area covers the central part of The Netherlands (40 by 60 km centered at 52.19° N, 5.91° E). This area was selected considering both the heterogeneity of the landscape and the availability of cloud free imagery. A Landsat TM-5 image acquired on 10 July 2003 and a time series of seven MERIS full resolution level 1b images acquired between February and December 2003 were used to illustrate the proposed data fusion approach.

The TM image was already geo-referenced to the Dutch national coordinate system (RD) and had a pixel size of 25m. The MERIS FR images were first corrected for the smile effect [4] and then they were transformed into top of atmosphere radiances (L_{TOA}) using the metadata provided with the files. Figure 1 shows, as an example,

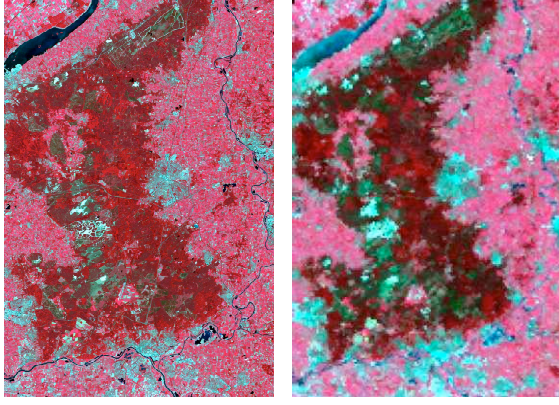


Figure 1. Study area: RGB composite of the Landsat TM image from the 10th July (left) and the MERIS FR image acquired the 14th July (right)

an RGB composite of the Landsat TM and the MERIS FR images acquired in July 2003.

2.2. Co-registration and PSF effects

One prerequisite when combining different kinds of images is to have them perfectly co-registered. Commonly, this is achieved by transforming the images to a common coordinate reference system. This transformation implies re-sampling of the images which, in turn, might have adverse effects on the quality of the fused images. The simplest and fastest re-sampling method is nearest neighbour which preserves original pixel values but lacks geometric accuracy because the measurements are actually shifted to the nearest grid point. Other techniques, such as bi-linear or bi-cubic interpolation are more accurate in respect of the geometrical transformation. However, they produce synthetic pixel values. Because of these drawbacks, here we decided to use a different approach: the actual GIFOV of each MERIS pixel will be computed. In order to use geo-location values that are as accurate as possible we used the AMORGOS tool [5].

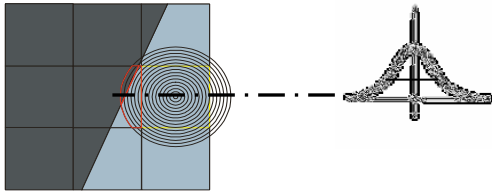


Figure 2. PSF effects: GIFOV of a pixel (left) and spatial response along cross-sectional view (right)

This tool calculates the geographic coordinates (WGS84) of the center of each pixel in the MERIS image based on satellite telemetry (ephemerides, look

angles) and the reference ellipsoid. Based on this information we determine the extent (i.e. the corner coordinates) of each MERIS pixel. However, because of the blurring of the signal due to the sensor PSF also spectral signatures of areas actually outside the GIFOV of the low resolution pixel contribute to its signal [6].

According to [7] the effective point spread function (PSF_{tot}) of an imaging system consists of several components: (1) the signal is blurred within the optical system (PSF_{opt}), (2) motion of the sensor (PSF_{mot}) causes blurring in the in-track and/or cross-track direction (depending on the type of sensor), (3) the signal is integrated over the non-zero area of the detector element (PSF_{det}) and (4) the electronic components cause smoothing by applying a low-pass filter to reduce noise (PSF_{el}). By assuming that every component is a shift-invariant linear system, PSF_{tot} can be computed by convolution of its parts:

$$PSF_{tot} = PSF_{opt} * PSF_{mot} * PSF_{det} * PSF_{el} \quad (1)$$

In our method we model PSF_{det} using a 2 dimensional rect-function, the remaining parts are combined to PSF_{com} . PSF_{com} is modelled by a 2-D Gaussian:

$$PSF_{com} = \frac{1}{2\pi ab} e^{\frac{-x^2}{2a^2}} e^{\frac{-y^2}{2b^2}} \quad (2)$$

Parameters a and b, i.e. the standard deviations of the Gaussian, determine the width of PSF_{com} in pixel units. Finally, we can write PSF_{tot} as [8]:

$$PSF_{tot}(x, y) = \left(\frac{1}{2\pi ab} e^{\frac{-x^2}{2a^2}} e^{\frac{-y^2}{2b^2}} \right) * \left[rect\left(\frac{x}{\Delta x}\right) \cdot rect\left(\frac{y}{\Delta y}\right) \right] \quad (3)$$

PSF_{tot} models the spatial response of the MERIS sensor and is used to weigh the fractional contributions of the different landcover types, as obtained from the unsupervised classification of the TM image, to one MERIS pixel.

2.3. Data fusion

The unmixing-based data fusion approach, also known as spatial unmixing, is based on the linear mixing model. In contrast to the spectral unmixing, which is solved per pixel and for all bands at once, the spatial unmixing is solved for all the pixels at once but for one band at a time. The method can be summarized as follows:

First the TM image is classified into a number of classes (nc). Here we selected $nc=10, 20, 40, 60, 80$ and 100 classes and we used an unsupervised ISODATA classification rule. In this way, we can characterize our study area with different degrees of detail.

Secondly, the TM classified images are used to compute the fractional composition of each MERIS FR pixel (c.f. section 2.2). This step resulted in 168 fractional matrices (7 MERIS dates, 6 TM classification levels and 4 PSF σ values).

Thirdly, a spectral response is computed for each of the nc classes by solving the following equation for all MERIS bands and dates and PSF σ values:

$$\mathbf{P}_{(npx1)}^i = \mathbf{F}_{(npxnc)} * \mathbf{M}_{(ncx1)}^i + \mathbf{E}_{(npx1)}^i \quad (4)$$

where: \mathbf{P}^i is a vector that contains all the np MERIS pixel values for the band- i ; \mathbf{F} is the fractional matrix; \mathbf{M}^i is the (sought) vector of spectral signatures (band- i) for the nc classes

Notice that this system of equations is solved for each band independently and that a constrained least-squares method was used in order to solve the mixing equations. A constrained method was needed because the solution of the unmixing should fulfill the following two conditions: i) all the “endmembers” (MERIS radiance values) have to be positive and ii) they have to be equal or smaller than the (per band) MERIS radiance saturation values (EO helpdesk, personal communication).

Finally, we generated a series of fused images by substituting each of the TM classified pixels by its corresponding spectral signature. Because Eq. 4 was solved for all the fraction matrices, a total of 168 fused images were generated.

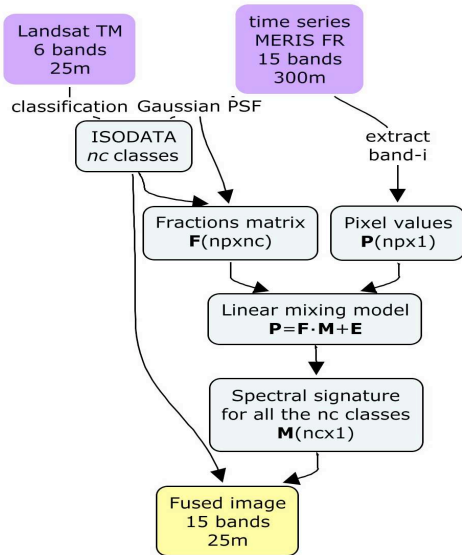


Figure 2. General scheme

2.4. Data fusion quality

A quantitative quality assessment of all the fused images was performed to find the combination of nc and

σ that produces the best spectral image. The so-called spatial ERGAS was used to compare the TM bands with its spectrally corresponding bands from the fused images. The spatial ERGAS index is computed as follows:

$$Spatial\ ERGAS = \frac{h}{l} \sqrt{\frac{1}{N} \sum_{i=1}^N (RMSE_i^2 / TM_i^2)} \quad (5)$$

where: h is the resolution of the Landsat image; l is the resolution of the MERIS image; N is the number of spectral bands involved in assessment (4 in our case); TM_i is the mean value of the TM band- i and $RMSE_i$ is the root mean square error computed between the TM image and its spectrally corresponding band from the fused images (for the band- i).

The quality of the fused images was also evaluated using the mean coefficient of correlation between the TM and the spectrally corresponding bands from the fused images:

$$CC_i = \frac{COV(TM_i, FUSED_i)}{\sigma_{TM_i} \cdot \sigma_{FUSED_i}} \quad (6)$$

$$MeanCC = \frac{\sum CC_i}{nbands} \quad i = 1, 2, \dots, nbands$$

where: CC is the coefficient of correlation for band- i , COV means covariance and σ is the standard deviation for the band- i of the TM and its spectrally corresponding band from the fused image.

3. RESULTS

3.1. Data fusion quality

Figure 3 summarizes the quality assessment of the 168 fused images. The top row illustrates the results for the spatial ERGAS: the temporal evolution (left) and the values for the images acquired in July (right). The lower the σ , the better the spatial ERGAS. For each σ series, the best spatial ERGAS was found for the image of July (i.e. the image that has nearly the same acquisition date as the Landsat TM data). The spatial ERGAS of the image of May seems too high when compared with the rest of the values. This might be because of differences in the phenological status, problems with the co-registration or because of residual cloud coverage. The effect of the number of classes used to classify the TM image is best seen for higher σ values. When looking at the images of July, we can see a steep decrease in the spatial ERGAS when moving from 10 to 20 classes. Later the values get more stable and $nc=80$ classes seems to produce the best results.

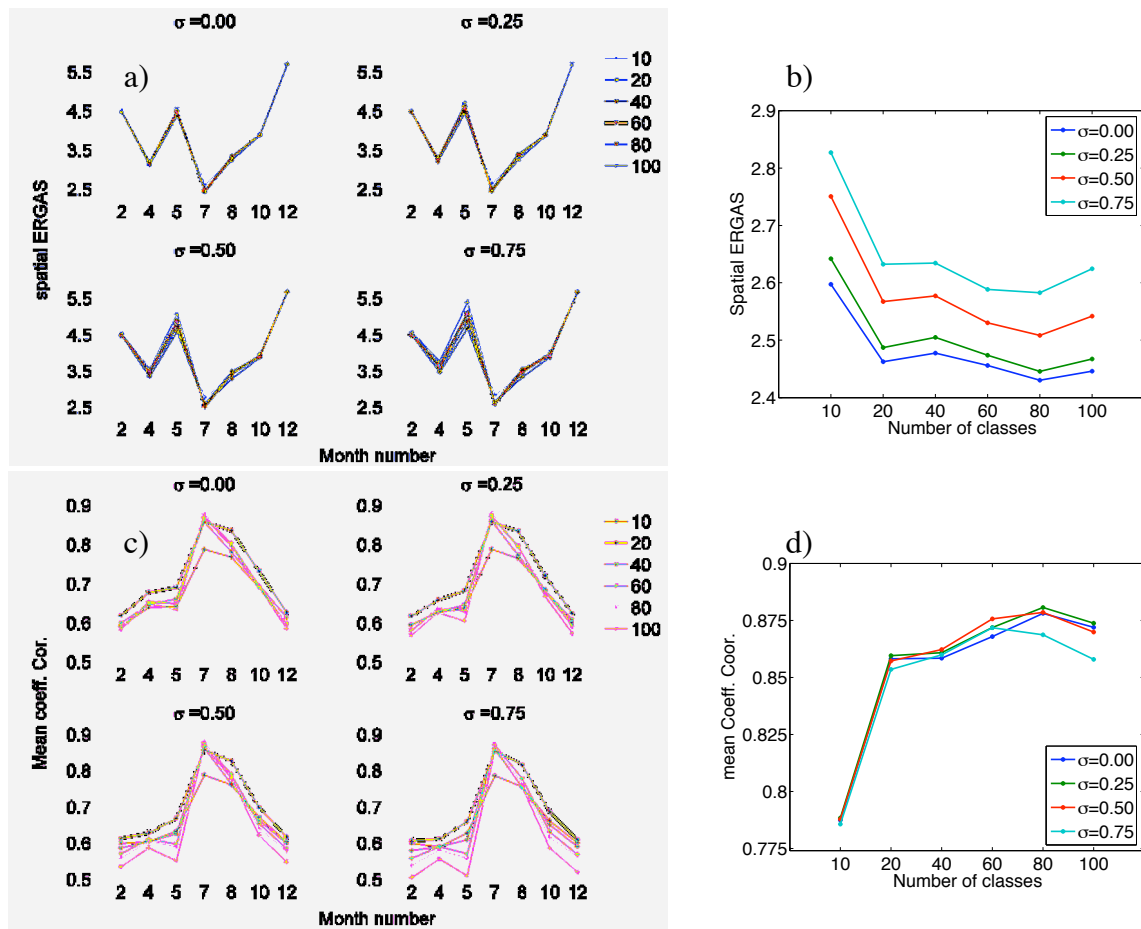


Figure 3. Quality assessment. Spatial ERGAS (top row) and coefficient of correlation (lower row) for the temporal series (left) and for the images acquired in July (right).

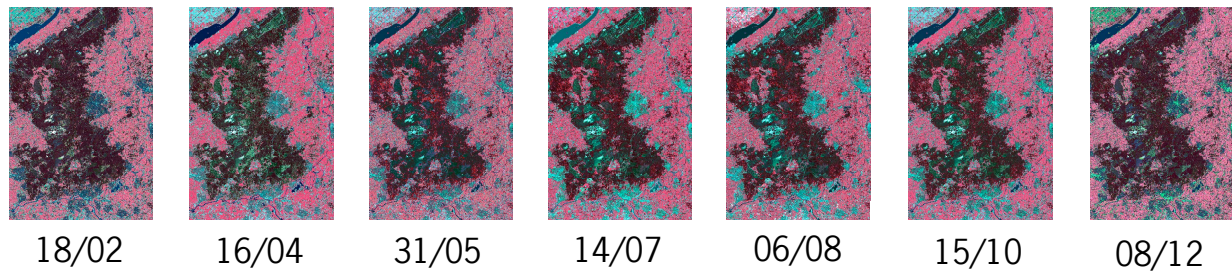


Figure 4. Temporal series of fused images for $\sigma=0.00$ and $nc=80$. Acquisition dates (day/month) of the MERIS FR data are indicated for each image.

Results for the coefficient of correlation (figure 3; lower row) were consistent with the spatial ERGAS assessment: best results were obtained for low σ values and for the images of July. For those images, using 80 classes gives the best coefficient of correlation. This time, $\sigma=0.25$ gives slightly better correlations. Nevertheless, the difference between the correlation coefficient obtained for $\sigma=0.00$ and for $\sigma=0.25$ is very small (notice the scale of the y-axis). Therefore, we decided to select as optimum parameters the ones that

we found for the spatial ERGAS quality assessment: $\sigma=0.00$ and $nc=80$.

3.2. Vegetation dynamics

The best series of fused images (figure 4) was first transformed from top-of-atmosphere (TOA) radiance to TOA reflectance (also known as planetary reflectance). The metadata provided with the images was used to perform this transformation. After that, the NDVI,

MTCI (MERIS terrestrial chlorophyll index) and MGVI (MERIS global vegetation index) vegetation indices were computed. The first one was selected because the NDVI is traditionally used to monitor vegetation dynamics. The MTCI and the MGVI were selected because these indices were specifically designed to monitor vegetation status using MERIS. The MTCI is linked to the total canopy chlorophyll content while the MGVI is related to the fraction of absorbed photosynthetically active radiation (FAPAR). The Dutch land use database produced for the years 2002 and 2003 (LGN5) was used to identify the location of the eight main land cover types in The Netherlands:

grassland, arable land, natural vegetation, water, coniferous forest, deciduous forest, built-up and bare soil (mainly sand dunes). A number of pixels belonging to these land cover types were selected to study the temporal evolution of the NDVI, MTCI and MGVI. The profiles were quite consistent for each land cover type. At the same time, some phenological variation could be identified when looking at different locations with the same land cover type. As an example, figures 5 and 6 show the temporal evolution of the NDVI, MTCI and MGVI. More specifically, figure 5 shows that the NDVI and MTCI have a very similar behavior. Most of the vegetated classes show a greenness/chlorophyll peak for

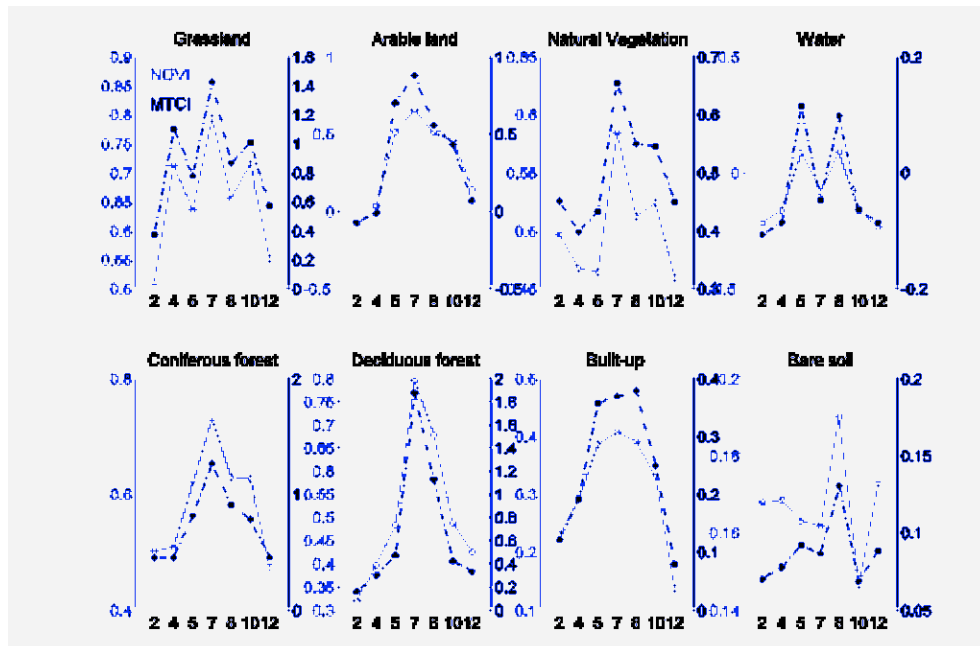


Figure 5. Examples of NDVI (left y-axis; full line) and MTCI (right y-axis; dash line) temporal profiles for the best series of fused images ($\sigma=0.00$ and $nc=80$). Month number is indicated in the x-axis.

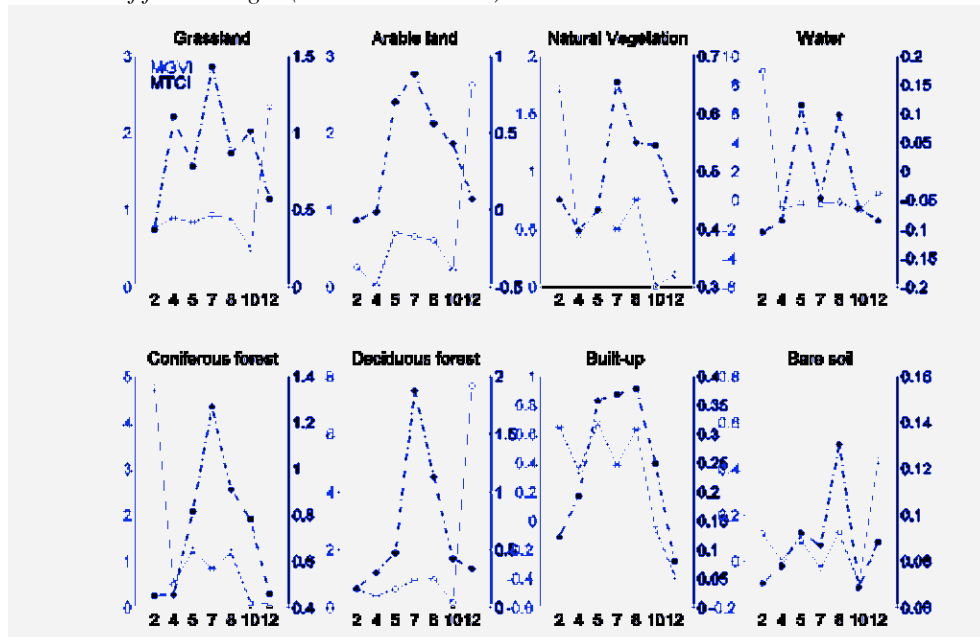


Figure 6. Examples of MGVI (left y-axis; full line) and MTCI (right y-axis; dash line) temporal profiles for the best series of fused images ($\sigma=0.00$ and $nc=80$). Month number is indicated in the x-axis.

the image of July. Non vegetated classes consistently present low values for both vegetation indices. In figure 6 we illustrate the temporal evolution of the two MERIS indices (the MTCI is also presented here for comparison purposes). The MGVI seems to provide consistent profiles for each of the land cover types under study if we exclude the values for the months of February and December (MGVI values are either too high or too low for those months).

4. CONCLUSIONS

In this work we have shown that the unmixing-based data fusion approach can be used to successfully downscale MERIS FR information to a Landsat-like spatial resolution. The AMORGOS tool was used to get accurate MERIS geo-location values. Good co-registration was achieved between the Landsat TM image and the temporal series of MERIS FR data.

Two parameters, namely the number of classes used to classify the Landsat TM image and the standard deviation of the Gaussian used to model the MERIS PSF were optimized using the results of the quantitative data fusion quality assessment. Results indicate a very small blurring effect for the MERIS sensor, i.e. a narrow spatial response. In fact, the impact of the sensor PSF on the method shown is rather small according to the results obtained. However, the sensitivity of the approach to the (unknown) PSF of MERIS will be a subject of further study.

The NDVI, MTCI and MGVI profiles extracted from the temporal series of fused images show consistent patterns for each of the land cover types under investigation. This creates new opportunities to monitor vegetation dynamics (phenology) at high spatial and temporal resolution.

ACKNOWLEDGEMENTS

The contribution of R. Zurita-Milla is granted through the Dutch SRON GO programme (EO-061). This work is also financially supported by the Austrian Science Foundation (*Fonds zur Förderung der wissenschaftlichen Forschung, FWF*), grant No. P17647-N04.

REFERENCES

- 1 L. Wald, Data Fusion Definitions and Architectures: Fusion of Images of Different Spatial Resolutions: Ecole des Mines Pres, 2002
- 2 Pohl and Van Genderen, Multisensor image fusion in remote sensing: concepts, methods and applications. International Journal of Remote Sensing. 19 pp. 823-854. 1998

- 3 B. Zhukov, D. Oertel, F. Lanzl, and G. Reinhackel, "Unmixing-based multisensor multiresolution image fusion," Ieee Transactions on Geoscience and Remote Sensing, vol. 37, pp. 1212-1226, 1999
- 4 R. Zurita-Milla, J. G. P. W. Clevers, M. E. Schaepman, and M. Kneubuchler, "Effects of MERIS L1b radiometric calibration on regional land cover mapping and land products.," International Journal of Remote Sensing. 28 (3-4) 653-673. 2007
- 5 ACRI-ST 2007, AMORGOS Software User Manual & Interface Control Document, rev. 0A.
- 6 E. P. Frans and R. A. Schowengerdt, 1997, Spatial-spectral unmixing using the sensor PSF, Proc. SPIE Vol. 3118, p. 241-249
- 7 R. A. Schowengerdt, 1997, Remote Sensing. Models and Methods for Image Processing; Second Ed., Academic Press.
- 8 G. Kaiser and W. Schneider, Estimation of Sensor Point Spread Function by Spatial Subpixel Analysis; IJRS (accepted for publication)